INL/CON-09-15331
PREPRINT

# CFD Investigation of Experimental Data Proposed to be a Validation Data Set

## ICONE 17

Richard W. Johnson

July 2009

The INL is a
U.S. Department of Energy
National Laboratory
operated by
Battelle Energy Alliance

Proceedings of the 17th International Conference on Nuclear Engineering
ICONE17
July 12-16, 2009, Brussels, Belgium

ICONE17-75604

# CFD INVESTIGATION OF EXPERIMENTAL DATA PROPOSED TO BE A VALIDATION DATA SET

**Richard W. Johnson**
Idaho National Laboratory
Idaho Falls, Idaho, USA

## ABSTRACT

The U. S. Department of Energy (DOE) is currently supporting the development of a next generation nuclear plant (NGNP). The NGNP is based on the very high temperature reactor (VHTR), which is a Generation IV gas-cooled reactor concept that will use helium as the coolant. Computational fluid dynamics (CFD) calculations are to be employed to estimate the details of the flow and heat transfer in the lower plenum where the heated coolant empties before exiting the reactor vessel. While it is expected that CFD will be able to provide detailed information about the flow, it must be validated using experimental data. Detailed experimental data have been taken in the INL's matched index of refraction (MIR) facility of a scaled model of a section of the prismatic VHTR lower plenum. The present article examines the data that were taken to investigate the suitability of such data to be a validation data set for CFD calculations. CFD calculations were made to compare with the MIR data to explore potential issues and make recommendations regarding the experiment.

## INTRODUCTION

One of the two competing designs for the VHTR is a prismatic or block configuration. (The other is a pebble bed design that employs thousands of tennis ball sized fuel pebbles, which collectively constitute the core). The prismatic-design VHTR core consists of dozens of hexagonal cross-sectioned blocks that are drilled for the fuel and attendant coolant flow channels. After flowing through the coolant flow channels in the blocks, the heated coolant exits the core into a lower plenum where it collects and flows out of the reactor vessel. Two concerns regarding the flow in the lower plenum are the impingement of hot coolant jets onto the lower plenum walls and the degree of thermal mixing of the helium coolant by the time it exits the reactor vessel. It is proposed that CFD simulations be made to estimate the desired local fluid flow and heat transfer details.

An important aspect of the application of CFD is to validate the results against detailed experimental data. For this purpose, a scaled model (1:6.55) of a section of the lower plenum of the prismatic VHTR reference design was built and installed in the Idaho National Laboratory's matched index of refraction (MIR) test facility to obtain detailed velocity and turbulence data [1]. Figure 1 provides a top view of the model showing the inlet jet ports and the cylindrical posts that represent support pillars in the lower plenum (holding up the core). The wedge at the right in Fig. 1 represents a portion of a hexagonal graphite block lining the lower plenum. Figure 2 is a drawing of the scaled model with the CFD coordinate system. The MIR facility uses mineral oil at a precise temperature to match the index of refraction of the quartz used to construct the model. With no change in the index of refracted light, it is straightforward to obtain optical velocity data. Extensive three-dimensional flow data were obtained using two-camera particle image velocimetry (PIV) [1]. Data were taken for two inlet jet Reynolds numbers, 4300 and 12,400. Preliminary calculations of the lower $Re_{jet}$ data have been made [2, 3] with mixed results. The present calculations are for the $Re_{jet}$ = 12,400 case.

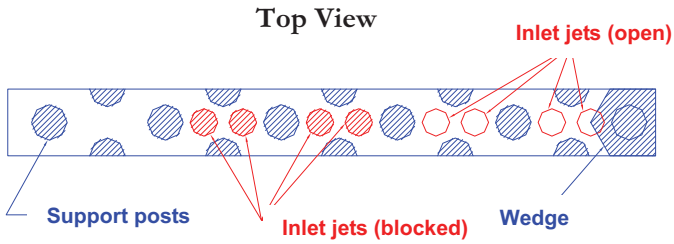


**Figure 1. Top view of the scaled model of a section of the prismatic VHTR lower plenum.**

The objective of the present investigation is to help raise and sort out issues about the suitability of the experimental data to be accepted as a validation data set. Some of the issues that

arise include the suitability of the model geometry itself, how many inlet jets should be employed, how sensitive the internal flow is to the symmetry/asymmetry of the inlet jets, how complex the flow actually is and what issues arise in the details of executing the CFD model. Three dimensional CFD calculations have been carried out to investigate these issues.

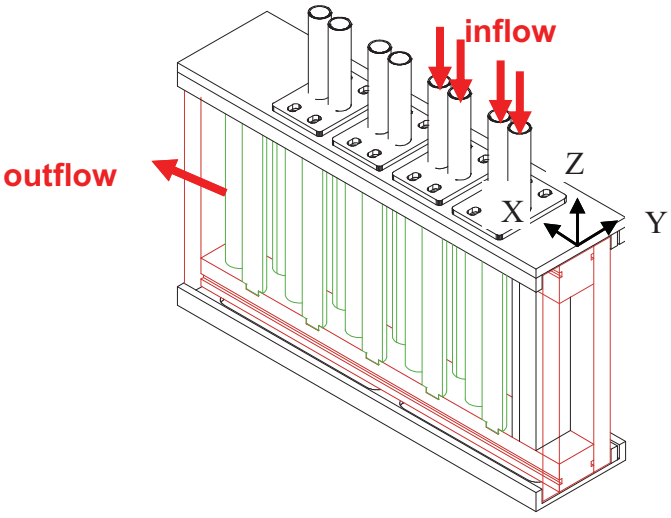


**Figure 2. Drawing of the scaled model.**

## CFD MODEL

The 104.8 mm wide scaled model shown in Fig. 2 was positioned inside the test section of the INL's MIR facility. The cross section of the MIR test section is 609.6 mm square. The mineral oil working fluid not only flows into the scaled model, but around the outside of the model as well (at a different velocity that inside the model). Consequently, the oil from the outer flow joins the oil from the inner flow at the model exit. A concern was raised that the outer flow would alter the flow at the exit of the scaled model, possibly affecting the flow inside the model. A two-dimensional study was performed to assess the affects of the outer flow on the inner flow to determine whether the outer flow would need to be included in the CFD model [4].

In the two-dimensional study, using the unsteady Reynolds-averaged Navier-Stokes (URANS) equations, called a URANS approach, the flow developed shedding vortices around the full and half cylinders included in the flow geometry. It was found [4] that because of the vortex shedding from the last full cylinder (at the left in Fig. 1) there is inflow at the exit plane of the scaled model. There was also found to be vortex shedding behind the 25.4 mm thick walls of the model. However, it was also found [4] that the flow profiles examined upstream of the last pair of half-cylinders inside the model were extremely close for the cases of computing only the inner flow using a 'pressure-outlet' outlet condition (employing the FLUENT commercial CFD code [5]) and that of including the outer flow in the computational domain. The pressure-outlet boundary condition simply sets the outlet pressure to be constant. While it is clear that this in not exactly correct, it is apparently fairly close to reality. Hence, the difference in flow between including or not including the outer flow, at least in the two-dimensional case, is confined to the region just inside of the model outlet. This result provided confidence for using only the flow domain inside the scaled model for the 3-D case, with a 'pressure-outlet' boundary condition.

In the previous study of the author [4], three different grids of increasing grid fineness were employed to check for grid independence. It was found that the intermediate and finest grid yielded very similar results. For the 3-D study, two two-dimensional grids were constructed based on the coarsest and intermediate grids from the 2-D study [4]. The meshes were then extruded in the vertical direction to obtain full 3-D grids. Additional inlet ports were added for the inlet jets. The number of cells allocated in the third dimension is 15 for the inlet jets and 125 in the body of the model. The mesh cells in the 3-D grid are hexahedral. The two 3-D meshes contain about 4 million cells and 14 million cells (grid b2), respectively. The commercial mesh software GAMBIT 2.4.6, which is bundled with FLUENT [5], was used to create the meshes.

The physical model on which the CFD model is based has an overall length of 485.42 mm, a width of 53.98 mm, and a height of 217.50 mm. The first two inlet jet ports have a height of 9.62 mm and the second two a height of 9.79 mm above the plane of the inlet. The plane of the inlet contains the origin of the coordinate system. The vertical direction (Z) is zero at the inlet plane, positive upwards. The origin for the streamwise direction (X) is actually 558.80 mm upstream of the outlet. The transverse direction (Y) is zero at the symmetry plane that divides the model in half vertically; see Fig. 2. Figure 3 illustrates the geometry of the 3-D meshes, showing the four active inlet ports (green), the half and full posts and the outlet plane (red); walls are grey. Figure 4 provides a closeup of the fine mesh at the inlet plane showing two of the inlet jets and the location of a display plane for contour plots of velocity that will be presented later.

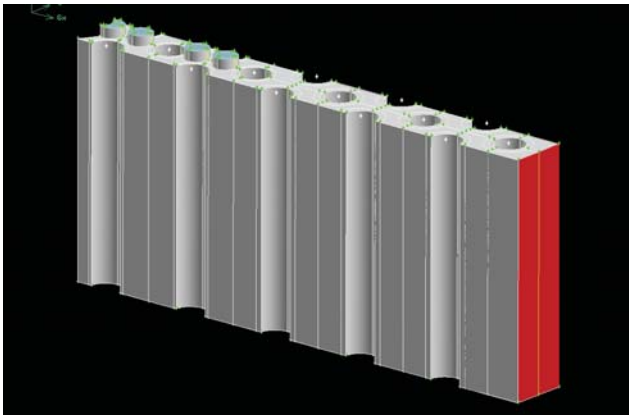

**Figure 3. Geometry of the extruded 3-D mesh.**

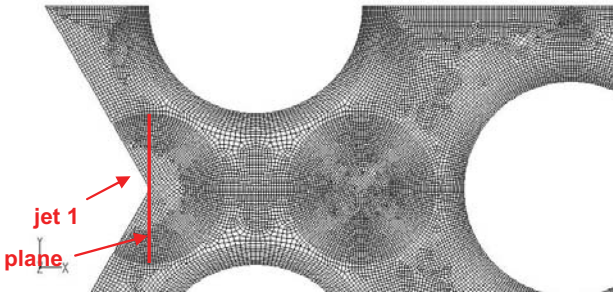


**Figure 4. Closeup of fine 3-D mesh including location of jet 1 and a display plane.**

The commercial CFD code STAR-CCM+ [6] is used for the 3-D computations, inasmuch as a large number of parallel licenses are available at the INL for its use. The flow problem is set up using a URANS approach, assuming that the flow is nonstationary (because of vortex shedding) as in the 2-D study [4]; it is also set up with constant fluid properties. Second-order differencing is used for both spatial and implicit temporal discretization; the segregated solver is used.

An earlier study by the author [7] of flow in a staggered tube bank indicated that the normal Reynolds stresses are anisotropic, requiring a turbulence model that permits such. The Reynolds stress model (RSM), which solves a differential equation for each Reynolds stress, was used therein. Inasmuch as the present geometry has similarities to the earlier flow [7], it was decided to use the RSM (with the linear pressure-strain option) for the present case as well. While the near-wall $y^+$ values range approximately from 1 to 20, which includes the viscous sublayer, the standard wall functions, which can accommodate the viscous sublayer, are used.

The initial simulations using the 14 million-cell mesh use a time step of $7.5 \times 10^{-5}$ sec., which was found to be sufficiently small in the 2-D study [4]. The pressure-outlet boundary condition is used at the outlet in conformance with the findings in Ref. [4]. The unsteady problem is initiated by first running a steady-state problem until the convergence rate slowed significantly, and then starting the unsteady run. The iterative convergence for each time step was set based on the calculation of a Poiseuille flow, which has an analytical solution. It was found from the Poiseuille flow calculation that a residual computed in STARCCM+ in the default mode is converged at a value of about $1 \times 10^{-4}$.

## RESULTS AND DISCUSSION

Unsteady calculations have been made for the 4 and 14 mil. cell meshes for uniform inlet conditions and for inlet conditions based on interpolated MIR inlet data for the three velocities and the turbulent kinetic energy. The uniform inlet conditions are based on the measured mass flows into each of the 4 jets. Turbulence inlet conditions for the uniform inlet case are $k = 0.01$ J/kg and $\varepsilon = 0.1$ J/kg-sec. Turbulent kinetic energy for the MIR inlet data is shown in Fig. 5; $\varepsilon$ is set to 1.0 J/kg-sec.

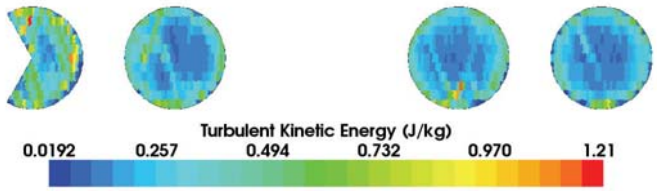


**Figure 5. Turbulent kinetic energy at jet inlets from MIR data.**

For the case of the MIR inlet data, the calculation eventually achieved a steady state condition. A separate calculation was made assuming a steady state case, which reached the same solution. For the 4 and 14 million cell uniform inlet cases, the calculations were approaching steady state.

Figure 6 illustrates a 3-D streamline computation from initial points located at the four jet inlets. Figure 7 is a photograph of a flow visualization test made by injecting air into jet 1 (at the far right) with mineral oil flowing into all four jets. It can be seen that the major flow features are present in the streamline figure that are present in the actual flow including a large recirculation region in the upper center of the flow, a smaller recirculation region at the lower right, a recirculation zone between jets 2 & 3, and flow that ascends gradually at the left after moving beyond the jets.

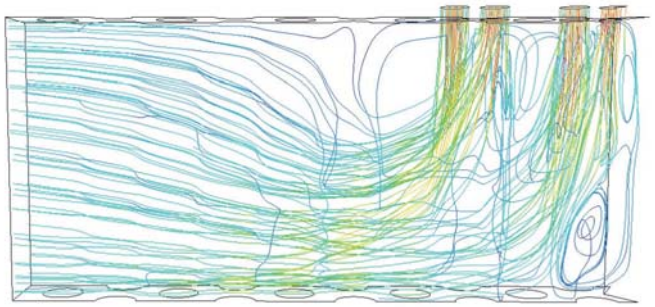

**Figure 6. 3D streamlines injected into the 4 jets.**

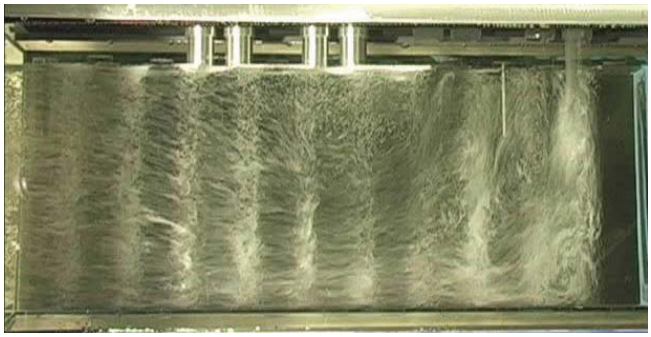

**Figure 7. Photograph of a flow visualization.**

Figure 8 illustrates contours of the vertical (Z) component of velocity for a plane normal to the X-direction that cuts

across jet 1 (see Fig. 4) for (a) the 4 mil. cell mesh, (b) the 14 mil. cell mesh, both using uniform inlet conditions, and (c) actual MIR data. Note the scales are matched. The fact that the jet is split is because of the presence of the wedge. As can be seen, the coarse mesh results shows the jet being moved to the left; the finer mesh results show the jet being moved to the right, but not so severely; and the MIR data show no movement either way, though there is some asymmetry in the velocity magnitude.

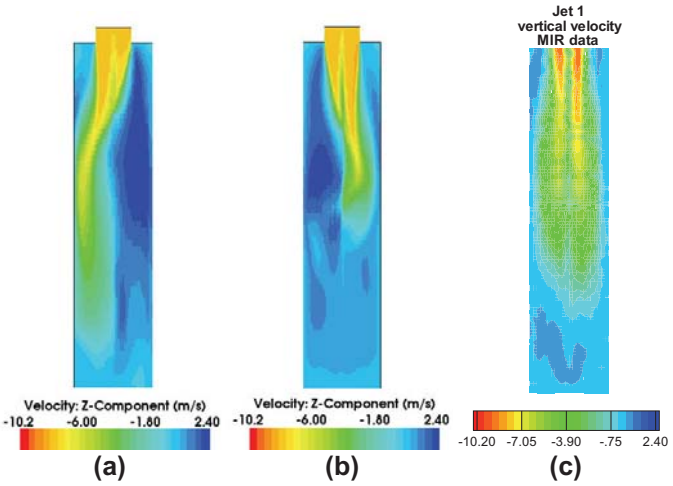


**Figure 8. Vertical velocity contours at a plane in jet 1, see Fig. 4, for (a) the coarse mesh, (b) the fine mesh, for uniform inlet conditions, and (c) the MIR data.**

Figure 9 shows vertical velocity contours for jets 2, 3 and 4 for planes normal to the X-direction along the centerline of each jet for the uniform inlet case for the 14 mil. cell mesh. Figure 10 shows vertical velocity contour plots for jets 2, 3 & 4 for the 14 mil. cell mesh case and using the MIR data for the inlets. Figure 11 shows contour plots of the actual MIR data for the vertical velocities for the same jets 2, 3 & 4. Note that the scales are all matched.

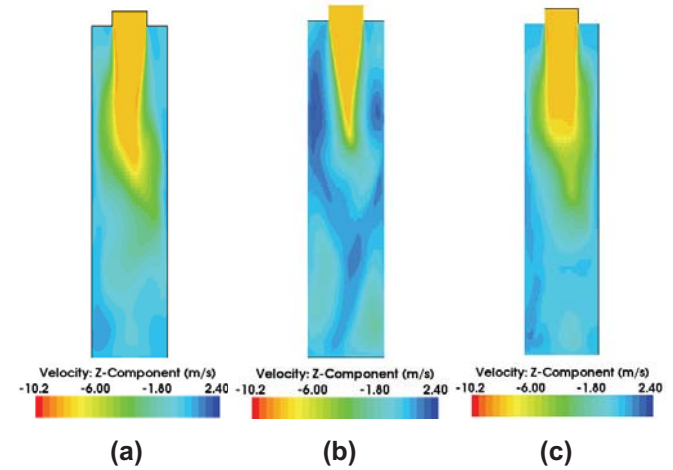


**Figure 9. Vertical velocity contours in planes normal to X for (a) jet 2, (b) jet 3 and (c) jet 4 for uniform inlet.**

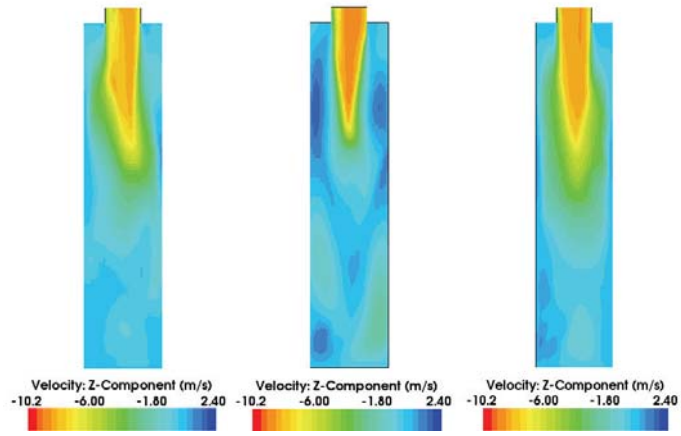


**Figure 10. Vertical velocity contours in planes normal to X for (a) jet 2, (b) jet 3 and (c) jet 4 using MIR data at the inlet.**

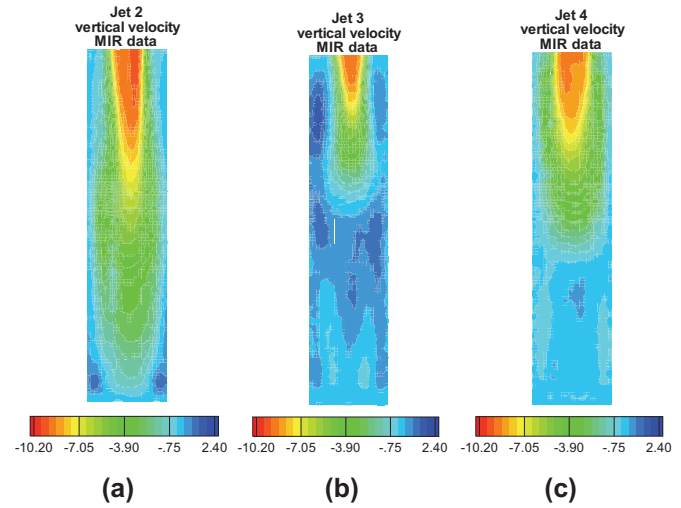


**Figure 11. Vertical velocity contours of MIR data for planes normal to X for (a) jet 2, (b) jet 3 and (c) jet 4.**

The actual MIR data for the inlet jets in the cross-plane are mostly symmetric in terms of 'shape.' The calculations, however, show significant asymmetry for jet 1, more so for the coarser mesh; however, the asymmetry is diminished for jet 2 and is minimal for jets 3 and 4. This seems to indicate that the wedge that protrudes into jet 1 may provoke some asymmetry, though the coarser mesh results of Fig. 8 also indicate that some of the asymmetry is because of mesh asymmetry itself. Inasmuch as similar meshing is used for all of the jets, it would seem that it is the presence of the wedge that perhaps intensifies the sensitivity of the flow to asymmetries in the mesh.

Figure 12 illustrates profile locations for data comparison. The profiles discussed in the following figures are for X and Y locations shown at either 70 mm or 150 mm below the inlet plane; for example, profile x1u is at location x1 at Z = –70 mm and x1d is at location x1 at Z = –150 mm.

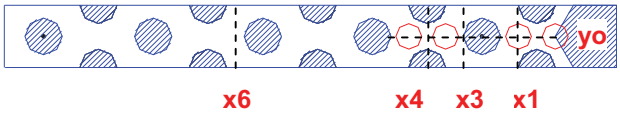


Figure 12. Locations of profiles for data comparison.

Figures 13 and 14 show profiles of vertical velocity along the centerline of the scaled model, profile 'yo' in Fig. 12, which bisects the centers of the four inlet jets at 70 mm and 150 mm below the inlet plane of the jets for the uniform inlet and MIR data inlet cases.

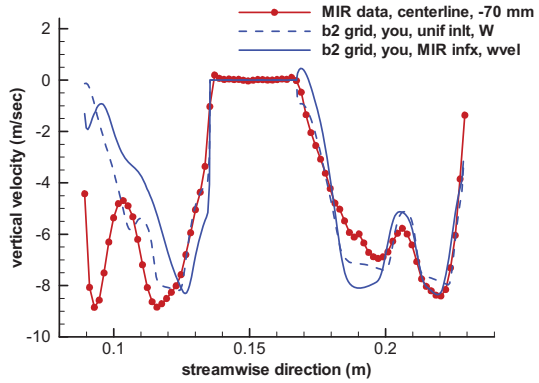


**Figure 13. Vertical velocity profiles for both cases along centerline at –70 mm compared to MIR data.**

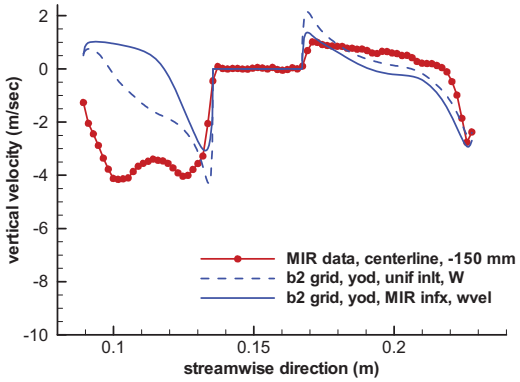


**Figure 14. Vertical velocity profiles for both cases along centerline at –150 mm compared to MIR data.**

In Figure 13, which compares profiles at 70 mm below the plane of the inlet jets, the signatures of the four jets can easily be seen in the MIR data. However, the profiles for both the uniform and MIR data inlet cases are dramatically incorrect for the first jet. Also, they both push the second jet somewhat downstream of the actual jet location. By the fourth jet, the MIR data inlet calculations closely follow the actual MIR data profile. In Fig. 14, at –150 mm, the signature of the first jet is still clear in the actual MIR data, but missing in both calculations.

Figure 15 provides a contour plot of the vertical velocity at the plane of symmetry (along the centerline) of the scaled model. It can be seen that jet 1 (at the left) is pushed forward by a recirculation zone that covers a region about half the height of the model. The flow visualization photograph, Fig. 6, clearly shows a recirculation zone in this region, but not so large. It may be the case that the turbulence model employed is not capturing the jet flow correctly for jet 1, which can be classified as a wall-jet. Interestingly, though the values for inlet turbulent kinetic energy and dissipation differ by about an order of magnitude for the uniform and MIR data inlet cases, jet 1 is still not captured correctly, though there are distinct differences. It seems that this is a separate effect that could be investigated separately from the rest of the flow field of the lower plenum. It may be the case that the wall-jet flow is not of concern to the final design of the lower plenum and that the wedge could be removed from a redesign of the model geometry.

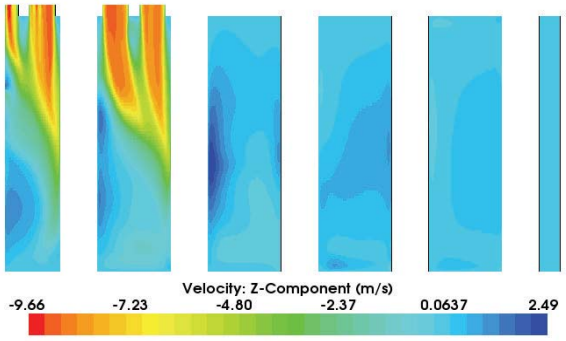


**Figure 15. Contour plot of vertical velocity on center-plane of model for MIR data inlet case.**

Examination of velocity profiles at various locations in the flow field yields additional insight about the actual flow field and about the calculations when compared to experiment. Figures 16-19 show profiles of mean streamwise (X-direction) velocity for the cases of uniform (dashed lines) and MIR data (solid lines) inlet conditions compared to the MIR data for four profile locations x1, x3, x4 and x6 at Z-coordinates –70 mm (u) and –150 mm (d); see Fig. 12 for profile locations.

The calculations for mean streamwise velocity at 'x1', Fig. 16, are considerably incorrect for both cases. The MIR data exhibit asymmetry as well as asymmetric downward spikes in the profiles. For profile location 'x3', Fig. 17, the calculations for both cases show fair agreement, except, again for some asymmetric spikes in the MIR data. Some credence to the actual presence of these spikes is given by the fact that they occur in about the same transverse locations and in the same sense for both elevations. Results for location 'x4', Fig. 18, show fair agreement for the MIR data inlet case, except for 'x4d' near Y = 0.08. The uniform inlet case results show an incorrect trend for 'x4u'. Finally, at profile location 'x6', Fig. 19, broad agreement for both cases is achieved. Both the calculations and the MIR data display asymmetries, more particularly for lower values of the X-coordinate. Agreement between calculations for both cases and experiment improves for higher values of the X-coordinate and is quite good at location 'x6.'

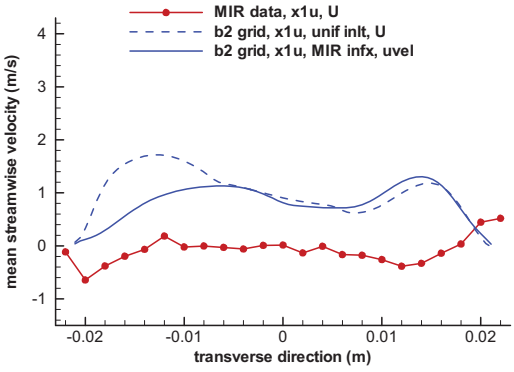


(a)

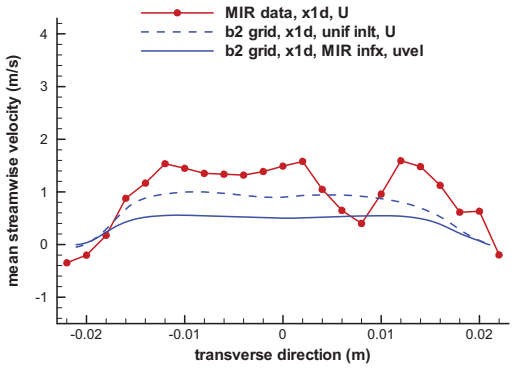


(b)

**Figure 16. Mean streamwise velocity at (a) x1u and (b) x1d**

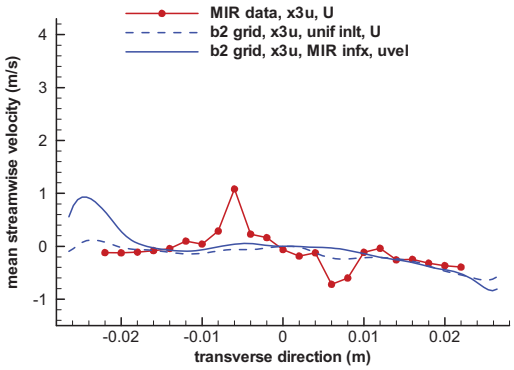


(a)

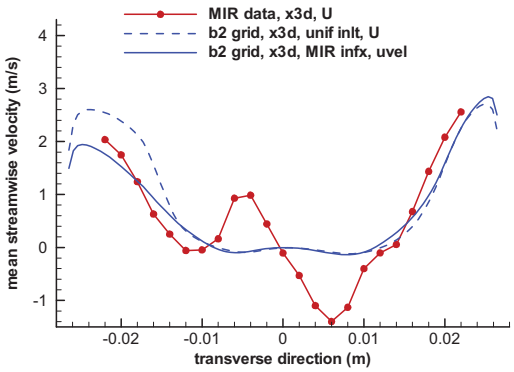


(b)

**Figure 17. Mean streamwise velocity at (a) x3u and (b) x3d**

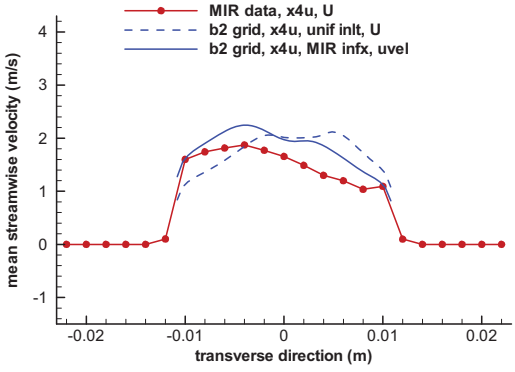


(a)

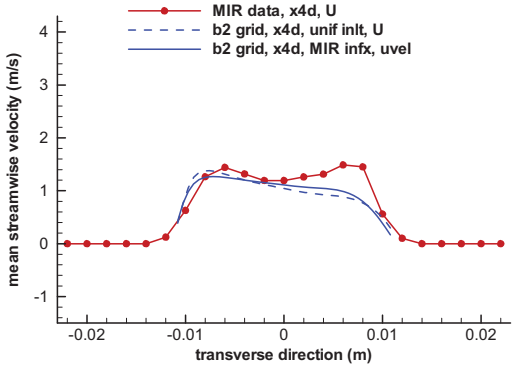


(b)

**Figure 18. Mean streamwise velocity at (a) x4u and (b) x4d**

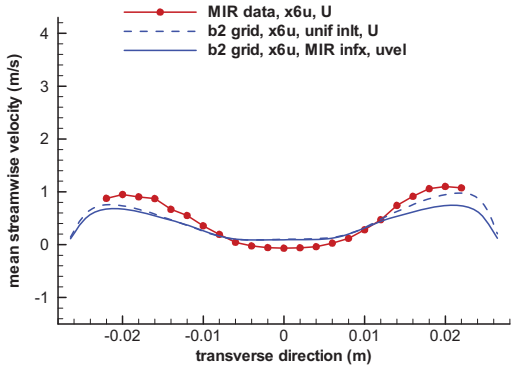


(a)

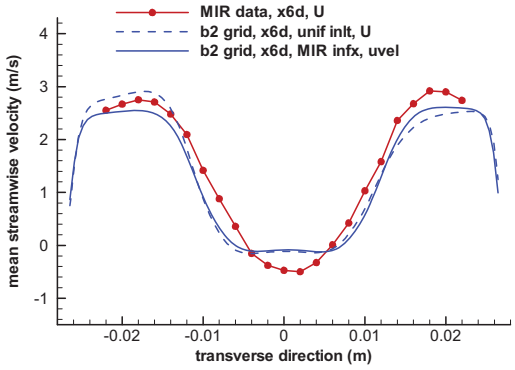


(b)

**Figure 19. Mean streamwise velocity at (a) x6u and (b) x6d**

Figure 20 provides contour plots for calculations for the MIR data inlet case of the mean streamwise velocity for horizontal planes at –70 and –150 mm. At –70 mm, Fig 20a, the asymmetry in the velocity is very apparent for lower values of X, but disappears for higher X values. At –150 mm, Fig. 20b, the asymmetry has diminished considerably, though some asymmetry is still present at low values of X.

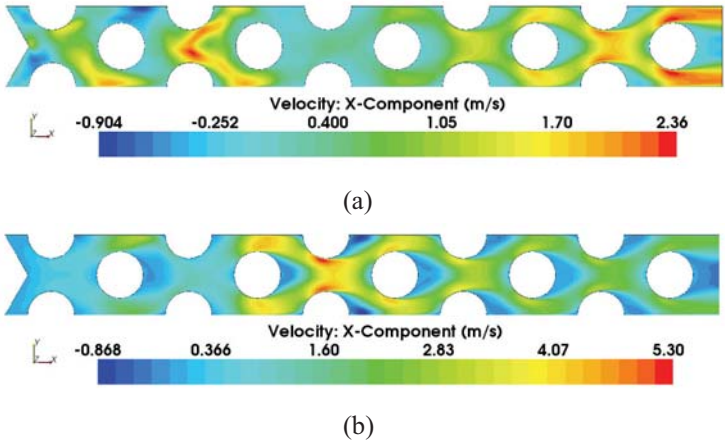


**Figure 20. Contours of calculations for the (steady) streamwise velocity for horizontal planes at (a) –70 mm and (b) –150 mm for MIR data inlet case.**

The above results indicate that significant disagreement between calculations and experiment occurs in the jet inlet region of the flow domain, particularly near jet 1. This disagreement could primarily be because the turbulence model is not doing a good job of calculating the wall jet that occurs at jet 1 with flow along the faces of the wedge. Inasmuch as this could be a serious inadequacy of the turbulence model, it would be good to look at wall jets separately from the rest of the flow dynamics. That is, a revised design for the present validation data set could be configured to have the wedge removed or the present geometry could be used with jet 1 blocked.

Figures 16-20 illustrate that there are asymmetries in the calculations for both computational cases and for the MIR data. However, the asymmetry is not the same for the calculations as for the data. The asymmetry in the MIR data is likely caused in part by some asymmetry in the inlet conditions. The fact that there are asymmetries in the inlet conditions for the four jets can be surmised by carefully examining the contour plots for the MIR data inlet case in Fig 11. However, it may also be that the asymmetry is simply very sensitive to slight variations between the actual and specified geometry or because of some other unknown factor. In view of the potential sensitivity of the symmetry of the flow to small or unknown factors, it is recommended that asymmetry be built into the model to greatly reduce the influence of small and unknown factors on the asymmetry of the flow. This could be done, for example, by offsetting the jets from the centerline. The actual asymmetry in the flow may also account for the poor agreement between experiment and the calculations in the upstream region of the flow domain. Also, building asymmetry into the flow may alleviate the need to construct a perfectly symmetric mesh to reduce the influence of numerical errors on the asymmetry of the calculations.

Another area of concern for the calculations is the fact that they exhibit backflow in a fairly sizable region of the outlet plane. This is because eddies are created by the full and half posts in the model and because there is a full post very near the outlet. Hence, it is recommended that the exit to the scaled model be extended further downstream or possibly that the last full post be removed. This would alleviate the fact that the calculations are probably not correct in the region just upstream of the outlet plane because the inflow conditions on the outlet plane are not really known and are very likely to be incorrectly represented by the CFD code.

It would be desirable to obtain additional data for cases where only one or two jets are operating. This would provide a data set that is less complicated that the present one and would be a good way to separate the various effects in the flow physics and the effects of turbulence models in computing them. Also, by plugging jet 1 or jet 1 & 2, the issue of the wall-jet could be avoided.

In the event of a redesign of the flow model, it would also seem to be desirable to employ only full posts inasmuch as only full posts are present in the lower plenum of the NGNP reference design. This would lead to a flow field that is closer to the actual field and that exhibits the actual mixing characteristics of the flow, which is one of the primary areas of concern for the flow in the lower plenum.

Finally, the issue of vortex shedding behind the full and half posts raises a concern. In the 2-D study [4], vortex shedding was clearly obtained for similar geometry. It could be the case that the strong asymmetry of the flow coupled with the narrow confinement of the flow has prevented vortex shedding in the calculations. It is the case that the MIR data do not capture vortex shedding because of the slow frequency of the data acquisition. It would be very desirable to have a PIV data acquisition system that could capture any vortex shedding. The author showed in Ref. [7] that there is a significant difference in the calculations for the tube bank flow assuming no vortex shedding and computing the vortex shedding. This issue of whether there actually is vortex shedding should be resolved by experiment.

## SUMMARY AND RECOMMENDATIONS

CFD calculations have been made of a scaled model of a small section of the lower plenum of the prismatic design of the next generation nuclear plant (NGNP), which is a gas-cooled very high temperature reactor (VHTR) and a Generation IV reactor concept. The flow field involves isothermal jets flowing vertically downwards into an open region populated with half and full cylindrical posts that represent core-support pillars in the lower plenum. It is found that both the experiment and the calculations exhibit asymmetry even though the geometry is symmetric. The calculations show the poorest agreement in the

region of the jet inlets, but improve as the flow carries on toward the exit with fairly good agreement with mean velocities closer to the flow exit. The asymmetry also is greatest nearer the jet inlets for both experiment and computations. The reason for the poor agreement near the jet inlets could be the inability of the turbulence model to predict flow along the wedge. It is concluded that this 'wall-jet' phenomenon should be examined as a separate effect, if it is present in the eventual design of the lower plenum. Recommendations in the event of a redesign of the model include using only full posts (not half posts), extending the exit to a greater length beyond the last post to avoid backflow and deliberately building in asymmetry into the model to prevent subtle and/or unknown effects from causing asymmetry. Experimental data could also be taken using only 1 or 2 jets, blocking off jet 1 to avoid the wall-jet issue to obtain additional data. It is also recommended to use a significantly faster data acquisition system to be able to definitively determine whether vortex shedding is present in the flow.

## NOMENCLATURE

| | |
|---|---|
| b2 | 14 million cell grid |
| CFD | computational fluid dynamics |
| DOE | U. S. Department of Energy |
| INL | Idaho National Laboratory, Idaho Falls, ID |
| k | turbulent kinetic energy |
| MIR | matched index of refraction |
| NGNP | next generation nuclear plant |
| PIV | particle image velocimetry |
| RSM | Reynolds stress transport turbulence model |
| URANS | unsteady Reynolds-averaged Navier-Stokes |
| VHTR | very high temperature reactor |
| $y^+$ | dimensionless wall distance |
| $\varepsilon$ | turbulent energy dissipation rate |

## ACKNOWLEDGMENTS

This manuscript has been authored by Battelle Energy Alliance, LLC under Contract No. DE-AC07-05ID14517 with the U.S. Department of Energy. The United States Government retains and the publisher, by accepting the article for publication, acknowledges that the United States Government retains a nonexclusive, paid-up, irrevocable, world-wide license to publish or reproduce the published form of this manuscript, or allow others to do so, for United States Government purposes.

## REFERENCES

[1] H. M. McIlroy, D. M. McEligot and R. J. Pink, Measurement of Flow Phenomena in a Lower Plenum Model of a Prismatic Gas-Cooled Reactor, Proceedings of the 16th International Conference on Nuclear Engineering (ICONE-16), Orlando, May 11-15, 2008.

[2] D. P. Guililen and H. M. McIlroy, Jr., Preliminary Study of Turbulent Flow in the Lower Plenum of a Gas-Cooled Reactor, Proc. NURETH-12, Pittsburg, PA, 2007.

[3] T. Gallaway, S. P. Antal, M. Z. Podowski and D. P. Guillen, NPHASE Predictions of Turbulent Flow in the Lower Plenum of a Prismatic Gas-Cooled Reactor, Proc. NURETH-12, Pittsburg, PA, 2007.

[4] R. W. Johnson, Development of a CFD Analysis Plan for the First VHTR Standard Problem, Proceedings of the 4th International Topical Meeting on High Temperature Reactor Technology (HTR2008), Washington, D. C., Sept. 28 – Oct. 1, 2008.

[5] FLUENT, version 6.3.26, 2008. FLUENT Inc., 10 Cavendish Court, Centerra Resource Park, Lebanon, NH, 03766.

[6] STAR-CCM+, version 3.04, 2008, CD-adapco, 60 Broadhollow Road, Melville, NY 11747.

[7] R. W. Johnson, "Modeling Strategies for Unsteady Turbulent Flows in the Lower Plenum of the VHTR," Nuclear Engineering & Design, **238**, pp. 482-491, 2008.